

# Journal of Materials Chemistry B

Accepted Manuscript



This is an *Accepted Manuscript*, which has been through the Royal Society of Chemistry peer review process and has been accepted for publication.

*Accepted Manuscripts* are published online shortly after acceptance, before technical editing, formatting and proof reading. Using this free service, authors can make their results available to the community, in citable form, before we publish the edited article. We will replace this *Accepted Manuscript* with the edited and formatted *Advance Article* as soon as it is available.

You can find more information about *Accepted Manuscripts* in the [Information for Authors](#).

Please note that technical editing may introduce minor changes to the text and/or graphics, which may alter content. The journal's standard [Terms & Conditions](#) and the [Ethical guidelines](#) still apply. In no event shall the Royal Society of Chemistry be held responsible for any errors or omissions in this *Accepted Manuscript* or any consequences arising from the use of any information it contains.

## ARTICLE

# A new fluorescent and colorimetric sensor for hydrazine and its application in biological system

Cite this: DOI:  
10.1039/x0xx00000x

Mingda Sun, Jing Guo, Qingbiao Yang,\* Ning Xiao and Yaoxian Li

Received 00th January 2012,  
Accepted 00th January 2012

DOI: 10.1039/x0xx00000x

www.rsc.org/

Hydrazine as a very important industrial chemical exhibits a high toxicity to the human beings. We here constructed a novel ICT-based fluorescence sensor with a high selectivity and sensitivity, rapid detection agents, and huge color-changing. We used the sensor for hydrazine determination in live cells and especially the live fish, and manufacture dipsticks with our sensor. The sensing mechanism is well rationalized with the aid of TD-DFT(time-dependent density functional theory) calculations.

## 1. Introduction

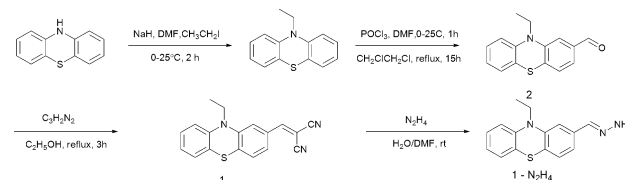
Hydrazine, as an important industrial chemicals, is widely used in various fields, such as pharmaceutical, chemical, involving catalysts and agricultural industries.<sup>1</sup> But due to its toxic for the human beings, hydrazine has been classified as a probable human carcinogen by the U.S. Environmental Protection Agency (EPA) with a low threshold limit value (TLV) of 10 ppb.<sup>2</sup> Hydrazine can cause critical damage to the kidney, liver and central nervous system of humans.<sup>3</sup> So in contrast to its value in industry, the toxic and carcinogenic effects it causes will lead to serious environmental contamination.<sup>4</sup> Therefore, the selective and sensitive detection of a trace amount of hydrazine has gained more and more attention.

To date, a variety of analytical techniques, including chromatography-mass spectrometric,<sup>5</sup> titrimetric,<sup>6</sup> spectrophotometry<sup>7</sup> and electrochemical methods<sup>8</sup> have been exploited for the purpose of hydrazine analysis.<sup>9</sup> Unfortunately, most of the methods mentioned before are costly, time consuming and complicated for real-time and on-site analysis. So simple but reliable detection methods for the rapid and sensitive detection of hydrazine both qualitatively and quantitatively are in great need.

In recent years, the fluorometric method has been extensively used to detect diverse analytes because of its selectivity, sensitivity, easy operation, economy and real-time detection.<sup>10</sup> Numbers of fluorescent sensors for hydrazine have been reported as of yet,<sup>11-16</sup> but most of the sensors invented up to now need pretty much organic solvent (>80%) in hydrazine detection and few of them work under neutral conditions,<sup>17</sup> which might be ascribed to the alkali chemical properties of hydrazine (pKa is 8.1) and the dilution effect on hydrazine concentration aroused due to the existing aqueous solvent.

Furthermore, analysis systems used in live cells especially in live animals have been rarely reported.<sup>18</sup> All these will definitely affect the application of the detection to some extent, especially in a physiological environment.

With the considering of all the above facts, we here developed a new fluorescent and colorimetric sensor. We constructed a sensor 1 with the introducing of malononitrile group as the electron acceptor and phenothiazine dye (compound 2) as the electron donor to form an ICT process. With the introducing of hydrazine, specific reaction between the arylidenemalononitrile and hydrazine group occurred and produced hydrazine,<sup>19</sup> which affected the intramolecular electron density distribution, followed by the changing of absorption and emission. Huge fluorescence enhancement (about 80-folds) provides a significant property for the hydrazine detection. Furthermore, our sensor can penetrate into live cells and especially the live fish. To the best of our knowledge, this is the first successful application of the fluorescent sensor for hydrazine in live animals.



**Scheme 1** Synthetic route of sensor 1 and the proposed mechanism for the response of 1 to hydrazine.

## 2. Experimental

### 2.1 Materials

Hydrazine hydrate, malononitrile and phosphoryl chloride were purchased from Sigma-Aldrich and used without any further purification. Phenothiazine and other starting materials commercially available were purified before using. All the other reagents were of analytical purity that used without further treatment. Respectively, aqueous Tris-HCl buffer (pH=7.4, 10 mM) solution was used as buffer to keep pH value.

## 2.2 Characterization

All the compounds prepared were characterized by electrospray ionization-mass spectrometry (ESI-MS), proton nuclear magnetic resonance ( $^1\text{H}$  NMR), and carbon nuclear magnetic resonance ( $^{13}\text{C}$  NMR).  $^1\text{H}$  NMR spectra of them were measured on a Bruker AV-300 spectrometer with chemical shifts reported as  $\delta$  [in  $\text{CDCl}_3$ , tetramethylsilane (TMS) as internal standard]. Absorption and luminescence spectra were obtained on a Shimadzu UV 2100 PC UV-visible spectrophotometer and a Hitachi F-4500 luminescence spectrometer, respectively. The pH values of the test solutions were measured with a glass electrode connected to a Mettler-Toledo Instrument DELTA 320 pH meter (Shanghai, China) and adjusted if necessary. All the measurement experiments were performed at about  $(298.0 \pm 0.2)$  K.

## 2.3 Synthesis

### Synthesis of Intermediate 3-Formyl-10- Ethylphenothiazine (2)<sup>20</sup>

Phosphoryl chloride of 6.0 g (39 mmol) was added slowly to 4 mL of dry DMF at 0 °C, and the mixture was stirred for 2 h at room temperature. A solution of 10-Ethylphenothiazine (4.3 g, 19 mmol) in 1,2-dichloroethane (25 mL) was added to it. After another 1 h, the reaction mixture was heated to 90 °C for 16 h. Then cooled and poured into 300 mL of water. After the solution was extracted with  $\text{CH}_2\text{Cl}_2$  (80 mL $\times$ 3) and dried with anhydrous magnesium sulfate, the solvent was removed and the residue was purified by column chromatography with petroleum ether/dichloromethane (1:1, volume ratio) as eluent to afford 3.45 g of compound 2 as a yellow solid, yield 70%,  $^1\text{H}$  NMR (400 MHz,  $\text{CDCl}_3$ ):  $\delta$  9.79 (s, 1H), 7.63 (d, J = 8.0 Hz, 1H), 7.57 (s, 1H), 7.16 (s, 1H), 7.10 (d, J = 6.2 Hz, 1H), 6.99–6.86 (m, 3H), 3.98 (d, J = 5.8 Hz, 2H), 1.46 (d, J = 5.4 Hz, 3H).  $^{13}\text{C}$ NMR (100MHz,  $\text{CDCl}_3$ ):  $\delta$ =12.87, 42.47, 114.39, 115.58, 123.26, 123.55, 124.47, 127.48, 127.59, 128.24, 130.18, 131.01, 143.08, 150.30; HRMS(ESI)  $m/z$   $[\text{M}+\text{H}]^+$  calc 256.0718, obs 256.0715

### Synthesis of Sensor(1)<sup>18</sup>

A solution of 2 (100 mg, 0.39 mmol) and malononitrile (39mg, 0.59 mmol) in ethanol (20 mL) was stirred at 85 °C for about 3 hours. The solvents was dried in vacuo and purified by silica gel column chromatography with  $\text{CH}_2\text{Cl}_2$  as eluent to yield g of compound 1 as a orange-red solid, yield 84%.  $^1\text{H}$  NMR (400 MHz,  $\text{CDCl}_3$ )  $\delta$  7.74 (dd, J = 8.7, 1.6 Hz, 1H), 7.54

(s, 1H), 7.48 (s, 1H), 7.17 (t, J = 7.8 Hz, 1H), 7.07 (d, J = 7.3 Hz, 1H), 6.98 (t, J = 7.5 Hz, 1H), 6.88 (dd, J = 15.8, 8.5 Hz, 2H), 3.98 (q, J = 7.0 Hz, 2H), 1.46 (t, J = 7.0 Hz, 3H).  $^{13}\text{C}$ NMR (100MHz,  $\text{CDCl}_3$ ):  $\delta$ =12.74, 42.73, 113.56, 114.46, 114.67, 115.68, 122.44, 124.15, 124.43, 125.16, 127.53, 127.84, 129.30, 131.50, 142.08, 150.30, 157.28; HRMS(ESI)  $m/z$   $[\text{M}+\text{Na}]^+$  calc 326.0830, obs 326.0838.

## 3. Results and discussion

### pH-Titration and Spectral Responses

We first investigated the effects of pH on the fluorescence intensity of 1 ( $5 \mu\text{M}$ ) in the absence and presence of hydrazine by controlling the pH of the mixed solution with buffer solution. From the Fig. 1 we could find that the fluorescence ratio ( $I/I_0$ ) of 1 showed no apparent changes with the pH from 2 to 12. But the fluorescence ratio of 1- $\text{N}_2\text{H}_4$  exhibited a slight decrease from 80 to 70 more or less when the pH increased to be 12. So considering environmental and biological applications, we chose the pH to be 7.4 as the testing system.

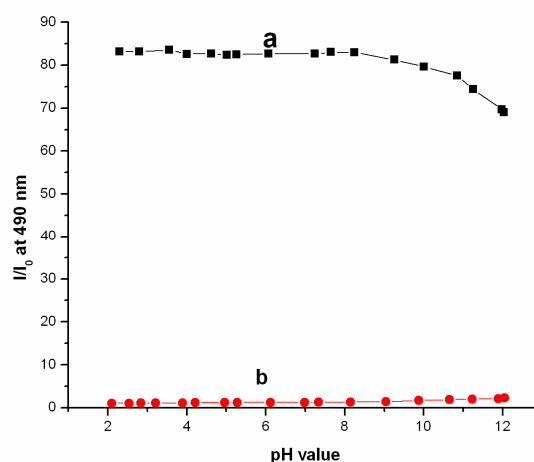


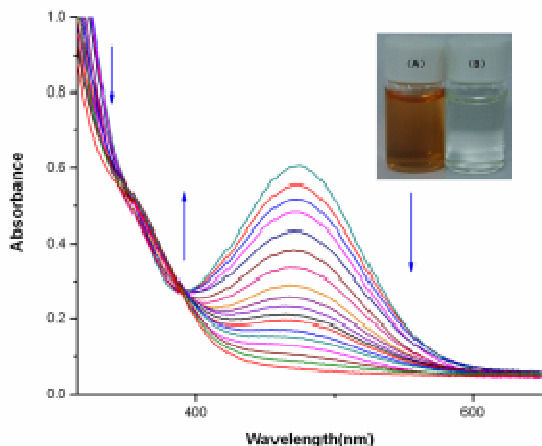
**Fig. 1** Fluorescence intensity ratio of sensor 1 in DMF-H<sub>2</sub>O (7:3, volume ratio) with (a) and without (b) hydrazine measured as a function of pH.

### Absorption spectral response

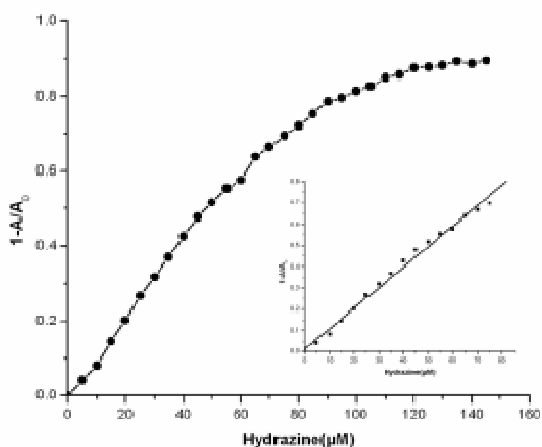
The changes of the UV-vis spectra for the sensor 1 in the absence and presence of hydrazine were investigated. Considering environmental and biological applications, we selected the solution of Tris-HCl buffer (pH=7.4, 10 mM)-DMF (3/7, v/v) as the testing system to investigate the optical response of 1 at room temperature. As shown in Fig. 2, 1 showed a main absorption band at 475 nm, which was attributed to the intramolecular charge transfer (ICT) transition in the molecular. Upon addition of hydrazine, the absorption intensity at 475 nm decreased evidently, whereas a weak new absorption peak appeared at 360 nm. With the hydrazine increased to be 3 equiv., the absorption intensity was found to

be the weakest at 475 nm. Such a strong reduction in the absorption behavior changed the color of the solution from orange to colorless as we can see in Fig. 6 (A), allowing the colorimetric detection of hydrazine by the naked eyes.

Fig. 3 shows the plot of  $[1-A/A_0]$  vs. the concentration of hydrazine, where  $A_0$  and  $A$  refer to the UV absorption intensity of aqueous solution of **1** at 475 nm in the absence and presence of hydrazine. Inset shows the linear relation for concentration of hydrazine in the range of 0-80  $\mu\text{M}$ . From the program we can find that  $[1-A/A_0]$  varies almost linearly vs. the concentration of hydrazine in the range of 0-80.0  $\mu\text{M}$ .



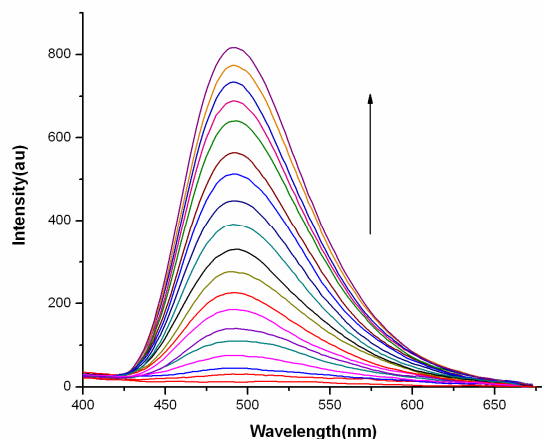
**Fig. 2** UV absorption spectra of sensor **1** (50  $\mu\text{M}$ ) in the presence of increased concentration of hydrazine (0-150  $\mu\text{M}$ ) in DMF-Tris-HCl buffer (10 mM, pH =7.4, 7:3, v/v); the inset shows the naked eye color change of sensor **1** with addition of hydrazine.



**Fig. 3** The plot of  $(1-A/A_0)$  at 475 nm vs. the concentration of hydrazine; inset shows the linear relation for concentration of hydrazine in the range of 0-80  $\mu\text{M}$ .

Next, the concentration dependent changes in the fluorescence spectra were investigated upon incubation of **1** (5  $\mu\text{M}$ ) with hydrazine. As shown in Fig. 4, **1** exhibited an extremely weak fluorescence and almost invisible under the fluorescent excitation at 490 nm. With the gradual addition of hydrazine, we could find the fluorescence at 490 nm increasing sharply, the addition of 4 equiv. of hydrazine to **1** induced a nearly 80-folds variation in the fluorescence ratio ( $I/I_0$ ) (Fig. 5). Fig. 6 (B) displayed apparently that after the addition of hydrazine, the fluorescence started to increase gradually from dark to blue.

We introduced a 3-methylenemalononitrile group into compound **2**, which can construct an ICT to form **1**. Significantly, the specific reaction between arylidene-malononitrile and hydrazine yielded the product of hydrazone, which interrupted the  $\pi$ -conjugation and affected the intramolecular electron density distribution, resulting in the UV absorption and fluorescence ratiometric responses to hydrazine in aqueous solution. Meanwhile, an obvious color changing from orange to colorless was also observed. The observation was in good agreement with the afore-mentioned design concept.



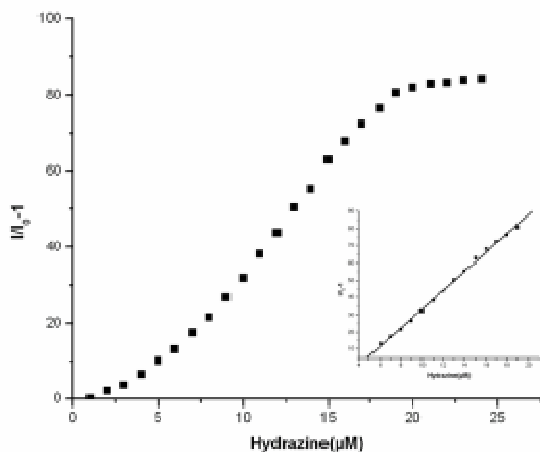
**Fig. 4** Fluorescence titration spectra of **1** (5  $\mu\text{M}$ ) in DMF-Tris-HCl buffer (10 mM, pH=7.4, 7:3, v/v) upon gradual addition of hydrazine. Excited at 350 nm, emission was monitored at 490 nm, slits: 5 nm / 5 nm).

Fig. 5 shows the plot of  $[I/I_0-1]$  vs. the concentration of hydrazine, where  $I_0$  and  $I$  refer to the fluorescence intensity of aqueous solution for **1** at 490 nm in the absence and presence of hydrazine. Interestingly,  $[I/I_0-1]$  varies almost linearly vs. the concentration of hydrazine in the range of 5.0-20.0  $\mu\text{M}$ , with the coefficient  $R=0.99846$ . This phenomenon implied that **1** was potentially useful for the quantitative determination of hydrazine concentrations.

The detection limit (DL) of **1** for hydrazine was determined from the following equation:<sup>14</sup>

$$DL = K \cdot Sb1/S$$

Where  $K = 2$  or  $3$  (we take  $2$  in this case);  $Sb1$  is the standard deviation of the blank solution;  $S$  is the slope of the calibration curve. Using this equation, we calculated the detection limit of hydrazine with **1** to be  $1.2191 \times 10^{-8}$  M. Note that this is much lower than the TLV (10ppb) set by the EPA.



**Fig. 5** The plot of  $(I/I_0 - 1)$  at 490 nm vs. the concentration of hydrazine; the inset shows the linear relation for concentration of hydrazine in the range of 5.0–20.0  $\mu\text{M}$ .



**Fig. 6** From left to right are photographs under visible light and fluorescence of **1** (10  $\mu\text{M}$ ) in DMF-Tris-HCl buffer (10 mM, pH=7.4, 7:3, v/v) with the gradual addition of hydrazine (0-4.0 equiv.).

### Selective and Competitive Experiments

To gain insight into the selectivity of sensor **1** for hydrazine, various anions of environmental and biological interests were introduced to investigate their impacts on the fluorescence response of **1**. Changes of fluorescence spectra of **1** (5  $\mu\text{M}$ ) caused by hydrazine (40  $\mu\text{M}$ ) and miscellaneous competing species (400  $\mu\text{M}$ ) (including  $\text{CN}^-$ ,  $\text{Br}^-$ ,  $\text{I}^-$ ,  $\text{N}_3^-$ ,  $\text{SCN}^-$ ,  $\text{NO}_3^-$ , EDTA,  $\text{CH}_3\text{COO}^-$ ,  $\text{H}_2\text{PO}_4^-$ ,  $\text{SO}_4^{2-}$ ) in DMF-Tris-HCl buffer (10 mM, pH=7.4, 7:3, v/v) were explored in Fig. 7. As could be seen from the diagram, these competitive species, which often showed strong interference in the hydrazine detecting did not

lead any significant fluorescence changes. The competitive experiments also showed that the fluorescence emission spectrum of **1** (5  $\mu\text{M}$ ) with hydrazine (20  $\mu\text{M}$ ) remained almost undisturbed with the inducing of excess competitive species. Some competitive metal ions were also investigated (Fig. S7, ESI).

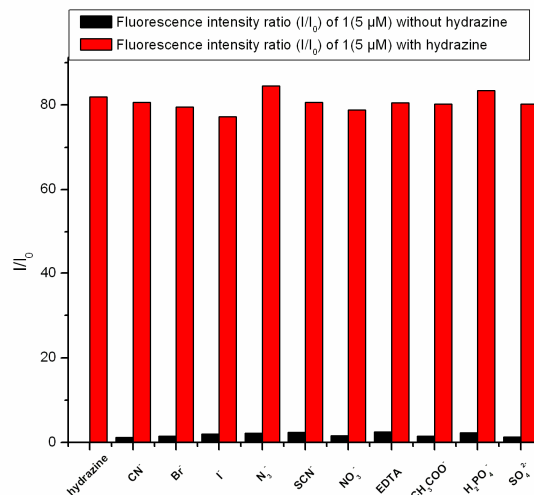


**Fig. 7** The fluorescence intensity ratio ( $I/I_0$ ) at 490 nm of **1** (5  $\mu\text{M}$ ) with various competing anions upon excitation of 350 nm. The competing anions are at concentration of 40.0 equiv. while hydrazine is 4.0 equiv..

### Detection of hydrazine in live cells

To further discuss the potential biological application of sensor **1**, we explored the capability of **1** to track the changes of hydrazine in live Hella cells (human neuroblastoma cells). The live cells were first incubated with **1** (10  $\mu\text{M}$ ) for 30 minutes at  $37^\circ\text{C}$  in 5%  $\text{CO}_2$  atmosphere, washed with phosphate buffered saline (PBS, pH=7.4, 7:3, v/v) three times. Then induced the hydrazine (40  $\mu\text{M}$ ) into the solution for 30 min. From Fig. 8 (A) we could observe extremely weak fluorescence in the cells which only treated with **1** (10  $\mu\text{M}$ ) under the fluorescence microscopy. However, as shown in Fig. 8 (B), the cells induced with hydrazine exhibited bright green fluorescence. From the pictures we could identify that **1** had successfully immersed into the cells and could track the intracellular hydrazine changing in live cells. The live cells imagings also demonstrated that **1** was membrane-permeable and could be a useful molecular sensor for studying the biological processes of involving hydrazine in live cells.

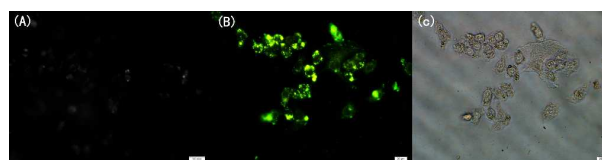


**Fig. 8** Fluorescence microscope imagings of live Hella cells with 1 (10  $\mu\text{M}$ ) before (A) and after (B) treated with hydrazine (40  $\mu\text{M}$ ) for 15 minutes. Bright-field transmission imagings of Hella cells incubated with 1 (10  $\mu\text{M}$ ) are shown in (C).

#### Detection of hydrazine in live fish

Zebra fish is a tropical freshwater fish. To further find out whether 1 can be used for visual detection of hydrazine in live animals, a series of experiments were carried out using the zebra fish as specimen. We feed the fish in the water with 1 (10  $\mu\text{M}$ ) dissolved in DMSO for 20 minutes, washed it with phosphate buffered saline (PBS, PH=7.4) and then observed it. The fish only exposed to 1 displayed almost no apparent fluorescence under 390 nm light (Fig. 9, A). But when we carried on to treat the fish with hydrazine (40  $\mu\text{M}$ ) for another 1 hour, as shown in Fig. 9 (B), a vividly illuminated green fish emerged with a beautiful contour and strong green fluorescence. The imagings demonstrated that our sensor 1 had successfully immersed into the fish body and from the fluorescence intensity we could suspect that the accumulations of the sensor in the gills, eyes and abdomen were higher compared to other parts of the fish body.<sup>21</sup>

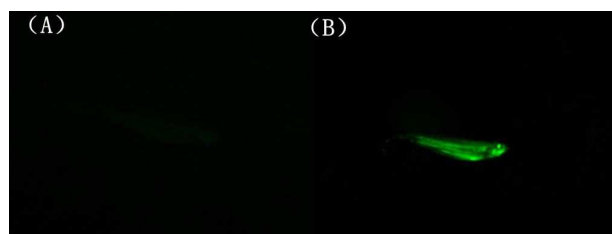


**Fig. 9** Imagings of full grown zebra fish under 390 nm light. (A) Fish incubated with only 1 (10  $\mu\text{M}$ ); (B) Fish incubated with 1 (10  $\mu\text{M}$ ) and then incubated with hydrazine (40  $\mu\text{M}$ ).

#### Applications

Significant attention has been paid to hydrazine owing to its effects on environmental toxins and human health problems, so easy and convenient testing methods in aqueous samples are in great need. We selected the filter paper to be the supporter of sensor 1 to make a dipstick for the hydrazine detecting. After dropping an aqueous solution of 1 on the neutral filter paper and drying it, we manufactured an orange red dipstick. Among the modified filter-paper exposed to the aqueous solution, only hydrazine induced the color fading from orange to colorless. And then we observed the dipstick under the 365 nm light, a bright fluorescence appeared compared with the previous dipstick without the hydrazine.



**Fig. 10** Color changes of test strips containing 1 treated with various anions from left to right (None,  $\text{I}^-$ ,  $\text{N}_3^-$ ,  $\text{SCN}^-$ ,  $\text{NO}_3^-$ ,  $\text{CN}^-$ ,  $\text{Br}^-$ ,  $\text{CH}_3\text{COO}^-$ ,  $\text{H}_2\text{PO}_4^-$ ,  $\text{SO}_4^{2-}$ , hydrazine, hydrazine under the light of 365 nm).

#### TD-DFT calculations

To get insight into the mechanism of the colorimetric and ratiometric fluorescence changes in the presence of hydrazine, TD-DFT (time-dependent density functional theory) calculations with 6-31G \* basis sets were carried out using a suite of Gaussian 09 programs for compound 1 and 1- $\text{N}_2\text{H}_4$ .<sup>22</sup>

As expected, for the compound 1, the TD-DFT calculations showed only one strong transition at 506 nm with an oscillator strength of  $f = 0.1332$  which corresponds to a HOMO  $\rightarrow$  LUMO (HOMO for the highest occupied molecular orbitals, LUMO for the lowest unoccupied molecular orbitals) transition. And for 1- $\text{N}_2\text{H}_4$ , calculations showed one strong transition at 337 nm with an oscillator strength of  $f = 0.1748$  which corresponds to a HOMO  $\rightarrow$  LUMO transition. TD-DFT calculations at the same level of theory indicated that the absorption band at the higher wavelength can be assigned to an ICT process. When we induced the hydrazine, the malononitrile group was removed resulting hydrazone, the ICT process from the phenothiazine to the malononitrile group through a two double bond spacer in 1 was altered. Simulated absorption spectra of 1 and 1- $\text{N}_2\text{H}_4$  obtained from calculations were in good agreement with the experimental results. It supported the experimentally obtained single band absorption spectrum of 1- $\text{N}_2\text{H}_4$ .

Comparing the level changes of the HOMO and LUMO in 1 and the corresponding hydrazone product 1- $\text{N}_2\text{H}_4$ , respectively, due to the ICT effect, after reaction with hydrazine both of them increased (Fig. 10), the LUMO increased much more. The HOMO  $\rightarrow$  LUMO energy gaps were calculated as 2.15 eV and 3.15 eV for 1 and 1- $\text{N}_2\text{H}_4$ . The energy gap between the HOMO and LUMO of 1- $\text{N}_2\text{H}_4$  was larger than that of 1. The calculations showed one emission at 487 nm for 1- $\text{N}_2\text{H}_4$ , which consistent highly with the experimental results of 490 nm. The calculations showed one emission at 735 nm for 1, well we had detected the emission at 740 nm for 1 too, but the emission intensity was so weak that we here did not discuss it.

The optimized structures for the ground state ( $S_0$ ) and lowest lying singlet excited state ( $S_1$ ) of 1 and 1- $\text{N}_2\text{H}_4$  were shown in the Fig. S8, ESI.

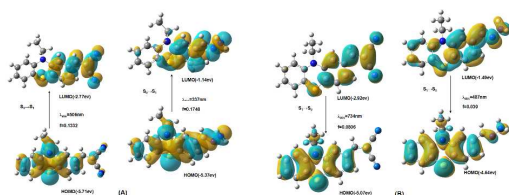


**Fig. 11** Frontier molecular orbitals involved in the vertical excitation (A) and emission (B) of sensors 1 and 1-N<sub>2</sub>H<sub>4</sub>.

## Conclusions

In summary, we here developed a new ICT-based fluorescence sensor by the conjugated of phenothiazine and arylidenemalononitrile groups with a good solubility in aqueous media. The sensor 1 displayed high sensitivity and selectivity for the hydrazine, with a color change from orange to colorless for the “naked-eye” detection. TD-DFT calculations suggested that the colorimetric and ratiometric sensing behavior was due to the ICT progress blocked by the inducing of hydrazine. Moreover, our sensor has an excellent biocompatible ability, and can indeed visualize the changes of intracellular hydrazine in live cells and especially in live fish. Dipsticks were also manufactured for the convenient detection. We expect our sensor a prospect in a range of chemical and biological applications.

## Acknowledgements

We acknowledge the Natural Science Foundation of China (No. 21174052) for the support of our work.

## Notes and references

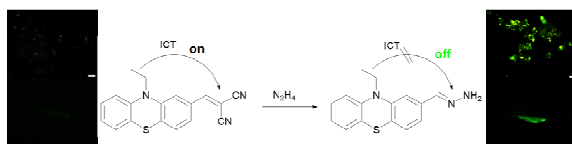
Department of Chemistry, Jilin University, Changchun 130021, P. R. China. Fax: +86431-88499576; Tel: +86431-88499576; E-mail: yangqb@jlu.edu.cn

† Electronic Supplementary Information (ESI) available: Supplementary Figures and Characterization of new compounds. See DOI:10.1039/b000000x/

- (a) U. Ragnarsson, *Chem. Soc. Rev.*, 2001, 30, 205–213; (b) S. S. Narayanan and F. Scholz, *Electroanalysis*, 1999, 11, 465–469; (c) K. Yamada, K. Yasuda, N. Fujiwara, Z. Siroma, H. Tanaka, Y. Miyazaki and T. Kobayashi, *Electrochem. Commun.*, 2003, 5, 892–896.
- A. Umar, M. M. Rahman, S. H. Kim and Y.-B. Hahn, *Chem. Commun.*, 2008, 166–168.
- (a) B. Toth, *Cancer Res.*, 1975, 35, 3693; (b) S. Garrod, M. E. Bollard, A. W. Nicholls, S. C. Connor, J. Connelly, J. K. Nicholson and E. Holmes, *Chem. Res. Toxicol.*, 2005, 18, 115; (c) C. A. Reilly and S. D. Aust, *Chem. Res. Toxicol.*, 1997, 10, 328.
- J. E. Troyan, *Ind. Eng. Chem.*, 1953, 45, 2608.
- (a) Y.-Y. Liu, I. Schmeltz and D. Hoffmann, *Anal. Chem.*, 1974, 46, 885; (b) J.-W. Mo, B. Ogorevc, X. Zhang and B. Pihlar, *Electroanalysis*, 2000, 12, 48; (c) S. D. Zelnick, D. R. Mattie and P. C. Stepaniak, *Aviat., Space Environ. Med.*, 2003, 74, 1285; (d) U. Ragnarsson, *Chem. Soc. Rev.*, 2001, 30, 205; (e) V. Andries and D. Couturier, *Mater. Perform.*, 2000, 39, 58.
- (a) Z. K. He, B. Fuhrmann and U. Spohn, *Anal. Chim. Acta*, 2000, 409, 83; (b) J. S. Budkuley, *Microchim. Acta*, 1992, 108, 103.

- (a) A. Safavi, F. Abbasitabar and M. R. Hormozi Nezhad, *Chem. Anal.*, 2007, 52, 835; (b) M. Mori, K. Tanaka, Q. Xu, M. Ikedo, H. Taoda and W. Z. Hu, *J. Chromatogr., A*, 2004, 1039, 135; (c) A. A. Ensafi and B. Rezaei, *Talanta*, 1998, 47, 645.
- (a) A. Benvidi, P. Kakoolaki, H. R. Zare and R. Vafazadeh, *Electrochim. Acta*, 2011, 56, 2045; (b) N. Maleki, A. Safavi, E. Farjami and F. Tajabadi, *Anal. Chim. Acta*, 2008, 611, 151.
- (a) A. Umar, M. M. Rahman, S. H. Kim and Y.-B. Hahn, *Chem. Commun.*, 2008, 166; (b) J. Liu, Y. Li, J. Jiang and X. Huang, *Dalton Trans.*, 2010, 39, 8693.
- (a) Zhang, J. F., Zhou, Y., Yoon, J., Kim, J. S. *Chem. Soc. Rev.* 2011, 40, 3416–3429; (b) Chen, X., Tian, X., Shin, I., Yoon, J. *Chem. Soc. Rev.* 2011, 40, 4783–4804; (c) Chen, X., Pradhan, T., Wang, F., Kim, J. S., Yoon, J. *Chem. Rev.* 2012, 112, 1910–1956.
- H. Falk and A. F. Vaisburg, *Monatsh. Chem.*, 1994, 125, 549–551.
- M. G. Choi, J. Hwang, J. O. Moon, J. Sung and S.-K. Chang, *Org. Lett.*, 2011, 13, 5260–5263.
- Y. Zhou and J. Yoon, *Chem. Soc. Rev.*, 2012, 41, 52–67.
- (a) R. Satapathy, H. Padhy, Y. H. Wu and H. C. Lin, *Chem. Eur. J.*, 2012, 18, 16061–16072; (b) H. J. Peng, W. X. Chen, Y. F. Cheng, L. Hakuna, R. Strongin and B. H. Wang, *Sensors*, 2012, 12, 15907–15946.
- (a) D. P. Elder, D. Snodin and A. Teasdale, *J. Pharm. Biomed. Anal.*, 2011, 54, 900–910; (b) Y. Zhu, J. Zhang and S. Dong, *Anal. Chim. Acta*, 1997, 353, 45–52.
- C. Batchelor-McAuley, C. E. Banks, A. O. Simm, T. G. J. Jones and R. G. Compton, *Analyst*, 2006, 131, 106–110.
- (a) S. Zhu, W. Lin and L. Yuan, *Anal. Methods*, 2013, 5, 3450; (b) Shyamaprosad Goswami, Sima Paul and Abhishek Manna, *RSC Advances*, 2013, 3, 18872; (c) Showcasing work from the laboratories of Prof. Jonathan L. Sessler and Prof. Jong Seung Kim, *Chem. Sci.*, 2013, 4, 4121.
- Jiangli Fan, Wen Sun, Mingming Hu, Jianfang Cao, Guanghui Cheng, Huijuan Dong, Kedong Song, Yingchao Liu, Shiguo Sun and Xiaojun Peng, *Chem. Commun.*, 2012, 48, 8117–8119.
- H. Falk and A. F. Vaisburg, *Monatsh. Chem.*, 1994, 125, 549–551.
- WANG Wei, ZHANG Ying-mu, LI Yao-xian and ZHAO Qing, *Chem. Res. Chin. Univ.* 2013, 29 (4), 632–637.
- Joydev Hatai, Suman Pal, Gregor P. Jose, and Subhajt Bandyopadhyay, *Inorg. Chem.*, 2012, 51, 10129–10135.
- Gaussian 09, Revision D.01*, M. J. Frisch, G. W. Trucks, H. B. Schlegel, G. E. Scuseria, M. A. Robb, J. R. Cheeseman, G. Scalmani, V. Barone, B. Mennucci, G. A. Petersson, H. Nakatsuji, M. Caricato, X. Li, H. P. Hratchian, A. F. Izmaylov, J. Bloino, G. Zheng, J. L. Sonnenberg, M. Hada, M. Ehara, K. Toyota, R. Fukuda, J. Hasegawa, M. Ishida, T. Nakajima, Y. Honda, O. Kitao, H. Nakai, T. Vreven, J. A. Montgomery, Jr., J. E. Peralta, F. Ogliaro, M. Bearpark, J. J. Heyd, E. Brothers, K. N. Kudin, V. N. Staroverov, R. Kobayashi, J. Normand, K. Raghavachari, A. Rendell, J. C. Burant, S. S. Iyengar, J. Tomasi, M. Cossi, N. Rega, J. M. Millam, M. Klene, J. E. Knox, J. B. Cross, V. Bakken, C. Adamo, J. Jaramillo, R. Gomperts, R. E. Stratmann, O. Yazyev, A. J. Austin, R. Cammi, C. Pomelli, J. W. Ochterski, R. L. Martin, K. Morokuma, V. G. Zakrzewski, G. A. Voth, P. Salvador, J. J. Dannenberg, S. Dapprich, A. D. Daniels, Ö. Farkas, J. B. Foresman, J. V. Ortiz, J. Cioslowski, and D. J. Fox, Gaussian, Inc., Wallingford CT, 2009.





A high selectivity and sensitivity fluorescent sensor for detection of hydrazine has been developed. It can trace the hydrazine changing in live cells and live fish. The sensing mechanism is well rationalized with the aid of TD-DFT calculations.